Published in final edited form as:
Cancer Res. 2011 March 1; 71(5): 1710–1720. doi:10.1158/0008-5472.CAN-10-3145.

Cancer Causes Cardiac Atrophy and Autophagy in a Sexually Dimorphic Manner

Pippa F. Cosper and **Leslie A. Leinwand**
Department of Molecular, Cellular, and Developmental Biology, University of Colorado at Boulder, Boulder, Colorado, USA

Abstract

Approximately one-third of cancer deaths are caused by cachexia, a severe form of skeletal muscle and adipose tissue wasting that affects men more than women. The heart also undergoes atrophy in cancer patients but the mechanisms and the basis for apparent sex differences are unclear. In a mouse colon-adenocarcinoma model, cancer causes a loss of cardiac mass due to a decrease in cardiac myocyte size that is associated with reduced levels of all sarcomeric proteins. Unlike skeletal muscle cachexia, atrophic hearts do not upregulate the ubiquitin-proteasome system (UPS) or its activity but increase autophagy. Thus, cancer causes cardiac atrophy by a mechanism distinct from that in skeletal muscle. Male tumor-bearing mice have a more severe phenotype than females, including greater cardiac mass loss and mortality, a more robust pro-inflammatory response to the tumor, and greater cardiac autophagy. In females, estrogen protects against cancer-induced cardiac atrophy and body weight loss by signaling through its receptor. Sex differences in cardiac atrophy need to be considered during the treatment of patients suffering from chemotherapy-induced cardiomyopathy to prevent exacerbation of cardiac dysfunction.

Keywords

cardiac muscle; atrophy; myosin heavy chain; sex; autophagy

Introduction

Cachexia is a severe form of skeletal muscle and adipose tissue wasting often associated with diseases such as cancer, sepsis, and AIDS. Cachexia affects approximately one-half of cancer patients and causes nearly one-third of cancer deaths (1). Weight loss is due to complex alterations in carbohydrate, lipid, and protein metabolism (2). The consequences of these metabolic changes include anemia, insulin resistance, production of acute phase proteins, and a negative nitrogen balance, which cannot be reversed with nutritional supplementation. These pathologic perturbations result in a significant loss of muscle protein, leading to pronounced muscle weakness and fatigue, increased sensitivity to infections, decreased responsiveness to both chemotherapy and radiation treatment and can ultimately lead to cardiac or respiratory failure (1).

There is a significant sexual dimorphism in muscle mass loss and survival in cancer patients. Multiple studies have found that male cancer patients lose more body weight and muscle mass than females and have shorter overall survival (3,4). Since cachexia increases mortality, it is likely that sex hormones are mediating these differences because post-

Corresponding author: Leslie A. Leinwand, Molecular, Cellular, and Developmental Biology, Room A417, UCB 354, Boulder, Colorado 80309, USA. Phone: (303) 492-7606; Fax: (303) 492-8907, Leslie.Leinwand@colorado.edu.

menopausal women lose their survival advantage, and estrogen therapy decreases colon cancer mortality (5,6).

Humoral factors secreted from or induced by the tumor are responsible for initiating skeletal muscle and body mass loss. Tumors induce a host immune response resulting in increased serum levels of pro-inflammatory cytokines, which cause skeletal muscle protein loss and cachexia *in vitro* and *in vivo* (7,8). Muscle mass loss can be due to increased protein degradation, decreased protein synthesis, or both (9), but cancer cachexia is primarily due to increased proteolysis (10). Cardiac and skeletal muscles utilize three major proteolytic pathways: the lysosome, Ca^{2+}-dependent calpains, and the ubiquitin-proteasome system (UPS). The UPS is responsible for the bulk breakdown of long-lived proteins and plays a major role in skeletal muscle protein degradation due to cancer (11). Components of the UPS are upregulated in the muscles of cancer patients and tumor-bearing rodents and inhibition of the UPS, but not the other proteolytic pathways, suppresses tumor-induced muscle proteolysis *in vitro* (12,13).

Cardiac muscle is labile and can undergo atrophy due to anorexia, prolonged bed rest, left ventricular assist device placement, and HIV (14–16). Given the high prevalence and mortality rate of cachexia and the fact that the heart is a striated muscle like skeletal muscle, it is surprising that relatively little attention has been paid to cardiac muscle atrophy in cancer patients. In 1968, Burch et al. observed that cancer patients had smaller hearts and decreased amplitude and duration of the QRS complex, implying functional defects (17). Cardiac atrophy in tumor-bearing rodents has also been observed (18), but the extent of cardiac muscle atrophy, functional implications, biochemical mechanisms and sex differences have never been fully characterized in any tumor model.

We have established a murine model of cancer-induced cardiac atrophy. Here we report that cardiac mass decreases rapidly during the course of tumor progression and there are multiple, significant differences in the disease phenotype between males and females. Males lose more body weight, skeletal and cardiac muscle than females and have a worse phenotype in all cardiac parameters we studied. We also show that cardiac atrophy is due to a decrease in all myofibrillar proteins, as opposed to myosin heavy chain (MyHC) specifically as reported in skeletal muscle cachexia (7). Most importantly, we provide data implicating autophagy as the main proteolytic pathway involved. To our knowledge, this report provides the first insight into this previously unappreciated aspect of cancer cachexia in both sexes and shows that the mechanisms of cardiac muscle atrophy are distinct from those in skeletal muscle.

Methods

Animals

CD2F1 (Balb/c X DBA2) is the mouse strain used in all cachexia studies. Colon-26 adenocarcinoma (C-26) (5×10^5 cells in 100 μL PBS) was injected subcutaneously into the right flank of 8-week old male and female mice. Echocardiography was performed as previously described (19). Serum from control and tumor-bearing animals was analyzed with a cytokine multiplex panel (Milliplex™, Millipore). Fulvestrant (ICI 182,780; Sigma) was dissolved in 70% ethanol and Cremaphor EL. Female mice were injected subcutaneously with 5 mg of ICI once weekly for 4 weeks starting the day of tumor cell inoculation. All animal studies were reviewed and approved by the Institutional Animal Care and Use Committee at the University of Colorado at Boulder.

Immunohistochemistry and Histology

Hearts were fixed in 10% buffered formalin and processed by Premier Laboratory (Longmont, CO). Slides were de-paraffinized and stained with Texas red-X conjugated wheat germ agglutinin (WGA) or anti-Cathepsin D (20) and analyzed with a Nikon Eclipse E800 microscope. For fibrosis analysis, slides were stained with picrosirius red, analyzed with polarized light microscopy (Zeiss Universal Microscope), and quantified with ImageJ.

Western blots and myofibrillar gels

For MyHC analysis, left ventricles were homogenized in high salt myosin extraction buffer (21). For other proteins, left ventricles were homogenized in 50 mM Tris pH 7.5, 150 mM NaCl, 50 mM NaF, 1 mM EDTA, 0.5% Triton X-100 (1% Triton for LC3 analysis) and complete protease inhibitor cocktail (Roche). MyHC antibodies were: MF20 (Developmental Studies Hybridoma Bank), anti-α-MyHC (BA-G5 hybridoma, ATCC) and anti-β-MyHC (VP-M667, Vector Laboratories). Other antibodies were: Anti-ubiquitin (Santa Cruz), caspase-9, LC3B, GAPDH (Cell Signaling Technology). Cardiac myofibrils were purified as previously described (22). Gels were loaded with equivalent percent of final heart weight (0.005%), stained with colloidal Coomassie Blue (ProtoBlue Safe, National Diagnostics), and analyzed with ImageJ.

RNA analysis

Total RNA was purified using TRI Reagent (Ambion) according to the manufacturer's protocol. cDNA was synthesized with Superscript II reverse transcriptase (Invitrogen) and random hexamer primers. Gene expression was determined by quantitative real-time reverse transcription PCR (qRT-PCR) using SYBR Green dye with gene specific primer sets and an Applied Biosystems 7500 Real-Time PCR system.

Caspase-3 and proteasome activity assays

Caspase-3 activity in cardiac lysates was determined as described (19). Proteasome activity assays were performed as described (23) with Suc-LLVY-AMC (Boston Biochem) as the substrate. Cleavage data was obtained over one hour and activity was determined by calculating the slope of the linear portion of the graph. Bortezomib (Velcade™) was kindly provided by Millennium Pharmaceuticals.

Ubiquitin conjugation assay

Briefly, left ventricular tissue homogenate (1 mg/mL) was incubated with 2 μg myc-Ub, 2 mM Energy Regeneration Solution, 50 μM MG-132, and 1 μM ubiquitin aldehyde (all Boston Biochem) at 37 °C for 30 minutes. The reaction was quenched with SDS-PAGE sample buffer. Ubiquitin-protein conjugates were detected by an anti-myc antibody (Cell Signaling).

Electron Microscopy

Electron microscopy was performed as described (20). Hearts were retrograde perfused with 2% gluteraldehyde in 0.1 M cacodylate buffer. Hearts were then post-fixed in 2% osmium tetroxide and 1% uranyl acetate for one hour each. Tissue was dehydrated using a series of ethanol washes, rinsed in propylene oxide and then a 1:1 mix of propylene oxide and Epon-Araldite epoxy resin. The tissue was then placed into Epon resin overnight, and polymerized at 60 °C for 48 hours. Sections were cut with a Diatome Ultra diamond knife, post-stained in 2% uranyl acetate and Reynold's lead citrate, and viewed using a Philips CM100 electron microscope.

Data and statistical analysis

Data are presented as mean ± SEM. Differences between groups were evaluated for statistical significance using Student's *t* test. *P* values less than 0.05 were considered significant.

Results

Cardiac atrophy caused by colon-26 adenocarcinoma is more pronounced in males than females

In order to define cardiac atrophy due to cancer and to determine whether there are sex differences, male and female mice were inoculated subcutaneously with colon-26 adenocarcinoma (C-26) cells, which cause a well-characterized cancer cachexia, resulting in rapid and severe skeletal muscle atrophy that is independent of anorexia (24). Male mice lost significantly more body weight than females at all time points studied (Figure 1A). Both male and female mice lost significant skeletal muscle mass at 15 days, and continued to lose muscle mass along the course of disease. The rate and extent of muscle mass loss was significantly greater in males than females (Figure 1B).

We measured cardiac mass at 15, 21, and 27 days post-tumor cell inoculum. Male mice lost 8.3% of their cardiac mass at 15 days, which progressed to 21.8% at 27 days (Figure 1C). Interestingly, female mice initially gained cardiac mass and lost only 9.8% by day 27. Males lost significantly more cardiac mass than females at days 15 and 27. The rate at which cardiac mass was lost also differed between the sexes (Figure 1C). This sexual dimorphism cannot be attributed to differences in tumor mass (Figure 1D). In addition to having less cardiac atrophy, female tumor-bearing mice survived about one week longer than males (data not shown).

Since pro-inflammatory cytokines contribute to skeletal muscle cancer cachexia (8), we performed a Mulitplex ELISA on male and female mouse serum at days 15 and 27. We found that males had a trend toward higher levels of pro- and anti-inflammatory cytokines than females (Supplementary Figure 1 and Supplementary Table 1), which correlates with findings in colorectal cancer patients (25). The enhanced inflammatory profile in male tumor-bearing mice may therefore contribute to the increased cardiac and skeletal muscle mass loss and decreased survival we observed.

Estrogen signaling is required for the maintenance of cardiac muscle mass in female tumor-bearing mice

Female cancer patients lose less skeletal muscle and body mass than men (3). Because we observed this in our mouse model, we determined if estrogen plays a role in the prevention of cardiac muscle mass loss in females by injecting female mice with Fulvestrant (ICI 182,780), a potent and specific estrogen receptor (ER) antagonist (26). Fulvestrant did not affect either cardiac mass or body weight in non-tumor-bearing mice (Figures 2A and 2C). Fulvestrant did, however, have a dramatic effect on tumor-bearing females. Inhibiting ER signaling caused female tumor-bearing mice to lose as much cardiac and body mass as tumor-bearing males (Figures 2B and 2D). The extent of skeletal muscle mass loss, however, was not significantly affected with Fulvestrant treatment nor was tumor mass. Hence, in this cancer model, estrogen signaling prevents cardiac muscle and total body mass loss.

Atrophic hearts have increased fibrosis and decreased aortic pressure and velocity

Cardiac fibrosis is often implicated in cardiac pathology and contributes to decreased function (27). In order to determine the extent of fibrosis in atrophic hearts, transverse

sections were stained with Picrosirius red, which reveals myocellular disarray and collagen deposition. We found that both male and female atrophic hearts had significant increases in fibrosis (50% and 65% respectively) and significant myocellular disarray (Figure 3A). Hearts from both control and tumor-bearing females had less (22% and 17% respectively) fibrosis than males but the fold change in fibrosis due to cancer was not significantly different between the sexes. Because collagen deposition and myocellular disarray cause myocardial stiffness and a decrease in cardiac function (28), we performed M-mode echocardiography on male and female mice at day 27. Male atrophic hearts had a significant 30% decrease in aortic pressure and a 16% decrease in aortic velocity (Figure 3B). Female tumor-bearing mice, however, did not have a decrease in any of the functional parameters studied (Figure 3B and Supplementary Table 2). Surprisingly, neither ejection fraction nor fractional shortening changed in either sex despite the extensive cardiac muscle loss.

Cardiac atrophy is due to a decrease in myocyte size, not an increase in cell death

Cancer-induced skeletal muscle atrophy is primarily due to increased protein degradation resulting in decreased myofiber size (10). Though apoptosis does occur in cachectic skeletal muscle, it does not significantly contribute to muscle mass loss (29). In order to determine how cardiac muscle atrophies in our mouse model, we first quantified myocyte size in male and female control and atrophic hearts (day 27). Cardiac myocyte cross-sectional area from male tumor-bearing mice was 31% smaller than male controls, while atrophic female myocytes were only 16% smaller than female controls (Figure 4A). The sexually dimorphic decrease in myocyte area correlates with the sex difference in cardiac mass loss.

To determine if increased cell death also plays a role in cardiac atrophy in males, we measured caspase-3 activity and the levels of caspase-9 cleavage products in cardiac muscle extracts and did not find an increase in either of these apoptotic markers at day 15 or 27 (Figures 4B and 4C). The amount of DNA per mg of tissue also did not change in atrophic cardiac muscle, while the amount of protein per mg tissue significantly decreased, as expected (Figure 4D). Together, these results indicate that cardiac muscle atrophy is due to a decrease in cell size, rather than an increase in apoptosis.

All sarcomeric proteins are equally decreased in atrophic cardiac muscle

Myofibrillar proteins make up 40% of left ventricular dry weight (30). Therefore, a decrease in myocyte size must be accompanied by a decrease in myofibrillar proteins. When the same percent of final heart weight was analyzed, we found that male atrophic hearts contained 22% less MyHC than controls (Figure 5A). Contrary to previous studies in skeletal muscle (7), we also found a significant decrease in sarcomeric actin that paralleled the decrease in MyHC (Figure 5A and Supplementary Figure 2A). MyHC/actin ratios therefore did not change, which suggests that entire cardiac sarcomeres are degraded during cancer-induced atrophy. To determine if all sarcomeric components decrease in parallel, we purified myofibrils from male atrophic and control hearts. When the same percent of final heart weight was loaded, we found a parallel decrease in all myofibrillar components (Figure 5B). Therefore, the absolute amounts of myofibrillar proteins decreased but the ratio of myofibrillar proteins in the sarcomere was maintained, presumably to preserve cardiac function.

Cardiac muscle contains two MyHC isoforms: α and β. The murine heart is primarily composed of α-MyHC, which has faster ATPase kinetics than β (31). A small increase in β-MyHC can cause decreased Ca^{2+}-activated ATPase activity and systolic function (32) and is a marker of pathology. qRT-PCR revealed that β-MyHC mRNA expression increased in both sexes at day 15, and significantly increased 16-fold in females and 22-fold in males at day 27 (Figure 5C).α-MyHC mRNA levels did not change in males but significantly

increased 3-fold in females at day 15, which correlates with the sex difference in cardiac mass at that time. In contrast to mRNA data, western blots revealed that α-MyHC protein decreased starting at day 15 and continued to decrease to 70% of control levels at day 27 in male hearts (Figure 5D). These results indicate that cardiac MyHCs are post-transcriptionally regulated, and suggest that increased protein degradation is responsible for the observed atrophy. Importantly, there was a significant increase in β-MyHC protein (Figure 5D and Supplementary Figure 2B), which is considered pathologic in the rodent heart.

The UPS is not upregulated in cancer-induced cardiac atrophy

Skeletal muscle atrophy is accompanied by increases in transcription of a common, specific set of genes that are involved in protein degradation by the UPS (33). Atrogin-1 and MuRF-1, muscle-specific E3 ubiquitin ligases, did not increase in male or female atrophic hearts, while expression increased 8-and 11-fold respectively, in the gastrocnemius of the same male animals (Figures 6A and 6B). Interestingly, the heart had 1.5- and 3-fold higher levels of atrogin-1 and MuRF-1 transcripts, respectively, than skeletal muscle and males had higher levels of these transcripts than females (Supplementary Figures 3A and 3B). Because the UPS is primarily responsible for skeletal muscle protein degradation (34), we quantified the levels of poly-ubiquitinated proteins in both the soluble and insoluble fractions of male cardiac muscle lysates and did not find significant differences at any time point (Figure 6C). Cachectic skeletal muscle has increased ubiquitination activity (35), but we did not find a change in ubiquitin conjugation activity in atrophic cardiac muscle at day 15 or 27 (Figure 6C). Additionally, proteasome activity in atrophic cardiac muscle lysates did not change at day 15 or 27, while it increased 2-fold in the gastrocnemius (Figure 6D). Together, these results indicate that unlike skeletal muscle, UPS activity is not upregulated in the hearts of tumor-bearing mice.

Autophagy is upregulated in atrophic hearts

Autophagy, a mechanism by which cells degrade large quantities of intracellular protein during periods of cellular stress, has been shown to play a larger role in the heart than in skeletal muscle (36). Cathepsin L, beclin, and LC3 (microtubule-associated protein 1 light chain 3) are well-characterized markers of increased lysosomal activation during myocyte atrophy and autophagy (37). Cathepsin L mRNA significantly increased 2-fold in both male and female atrophic hearts, while LC3 mRNA increased approximately 1.5-fold at day 27 (Figure 7A). Cytosolic LC3-I is lipidated to form LC3-II upon activation of autophagy. LC3-II is the only well-characterized protein that is specifically localized to autophagic vacuoles and serves as an accurate marker for autophagy (38). LC3-II protein levels were 7-fold higher in male atrophic hearts and only 3-fold higher in females at days 15 and 27 (Figure 7B). LC3-II was significantly higher in male than female hearts at day 27, which could explain the increased cardiac mass loss in tumor-bearing males. Direct evidence of autophagy was obtained by electron microscopy, which revealed the presence of numerous double-membraned autophagic vacuoles that contained portions of cytoplasm, mitochondria, and myelin-like structures (Figure 7C and Supplementary Figure 4B). Autophagic vacuoles were rarely detected at day 15, but were abundant by day 27. Additionally, atrophic hearts stained more heavily for cathepsin D, a lysosomal protease (Supplementary Figure 5). These results show that autophagy increases along the course of disease in cardiac muscle of tumor-bearing mice and is likely playing a major role in the enhanced protein degradation responsible for cardiac muscle atrophy.

Discussion

More than one-half of cancer patients suffer from cachexia, a severe muscle-wasting syndrome that results in decreased prognosis and survival (1). Cancer also causes cardiac muscle atrophy, a phenomenon that has been understudied by the scientific and oncology communities. A recent study found a direct correlation between muscle mass loss and death, and postulated that cardiac muscle atrophy contributed to the decreased survival in tumor-bearing mice (39). Our studies reveal the phenotype, mechanisms and sex differences of cardiac atrophy and show that it is distinct from skeletal muscle. Our results demonstrate that cardiac atrophy is an important feature of cancer cachexia that should be considered during the treatment and management of cancer patients, particularly in the setting of chemotherapy-induced cardiotoxicity or pre-existing heart disease.

We demonstrated that atrophic hearts had significantly decreased levels of all myofibrillar proteins. The issue whether sarcomeric proteins are selectively depleted is controversial; some have shown a specific decrease in MyHC (7), while others report that MyHC is not selectively lost in muscle atrophy (22). Although we show a parallel decrease in all sarcomeric proteins in the later stages of atrophy, it is possible that MyHC is specifically decreased early in cardiac atrophy, before any measurable mass loss. Presumably, absolute decreases in the number of sarcomeres would result in decreased cardiac function, which is why we were surprised to find that neither ejection fraction nor fractional shortening changed in either sex. However, other models of cardiac atrophy have also shown that atrophic hearts maintain their ejection fraction (40,41), implying that cardiac muscle is able to adapt functionally to muscle protein loss up to a certain point. We did find that male tumor-bearing mice had a significant decrease in aortic pressure and velocity, which correlates with clinical findings of hypotension in cancer patients.

The increases in β-MyHC we observed in the atrophic heart could have significant functional implications that may not be detected by echocardiography. β-MyHC induction in the rodent heart is pathologic and can contribute to myocardial contractile dysfunction since cardiac pressure development and power output decrease as β-MyHC increases (32,42). A more gradual model of cardiac atrophy might reveal higher levels of β-MyHC than we observed, which could affect cardiac function. Since cachexia in our mouse model is very rapid and leads to death in approximately four weeks, there may have been decreased cardiac function if the mice had lived longer. Because most cancer patients live with a tumor burden for many years, it is possible that cardiac abnormalities occur but likely remain undiagnosed due to insufficient monitoring.

The proteolytic pathways involved in skeletal muscle cachexia have been well-characterized and we were not expecting to find differences in the pathways upregulated in cardiac muscle. The UPS mediates skeletal muscle atrophy, but we did not find an increase in total ubiquitinated proteins, ubiquitin conjugating activity, or proteasome activity in atrophying cardiac muscle. The heart may not upregulate the UPS because it already has a high basal activity: cardiac muscle has a higher metabolic rate than skeletal muscle and has a higher protein turnover rate (43). Accordingly, expression of UPS components and proteasome activity are greater in cardiac than skeletal muscle (44). The baseline levels and activity of UPS components in the heart may therefore be sufficient to process the increased supply of substrates during cardiac atrophy.

Autophagy plays only a minor role in skeletal muscle atrophy (13), but we found a significant increase in autophagy in the hearts of tumor-bearing mice. Autophagy is essential for cardiac homeostasis and cardiac-specific reduction of autophagy results in contractile dysfunction, increased levels of polyubiquitinated proteins and increased apoptosis (45),

indicating that autophagy is important for protein turnover and clearance of misfolded or aggregated proteins. In fact, cardiac autophagy is induced in response to intracellular protein aggregates (46) and it is thought to be beneficial by removing aggregates that are unable to be cleared by the UPS. In addition to degrading mitochondria, it is possible that autophagosomes also degrade myofibrillar proteins cleaved from the sarcomere during cardiac atrophy in order to prevent protein aggregation and to preserve cardiac function. Although there is evidence for lysosomal degradation of myofibrillar proteins (47), it is a very controversial issue, and will be an important area of future investigation.

Cachexia increases mortality in both humans and rodents (39,48). Interestingly, male cancer patients have more severe cachexia and increased mortality than females (3,49). Accordingly, we found striking sex differences in cardiac and body mass loss and in all of our molecular analyses. We showed that ER signaling protects females against body weight and cardiac mass loss, indicating that estrogen could also be involved in the increased survival we observed in females. The increase in body mass loss we observed with Fulvestrant treatment must be due to increased fat loss since skeletal muscle mass was not affected. Female ERα knockout mice have increased skeletal muscle mass (50), which indicates that muscle mass is not positively regulated by ER signaling. Although decreases in estrogen are typically known to increase fat mass, the role of estrogen in regulating fat mass in a cachexia model is unknown, and will be an interesting area of future study. Collectively, these studies offer much-needed insight into the effects of cancer on the heart, and suggest that cardiac function in cancer patients, particularly in males, requires closer monitoring.

Supplementary Material

Refer to Web version on PubMed Central for supplementary material.

Acknowledgments

C-26 cells were a generous gift from Dr. Denis Guttridge, The Ohio State University. We would like to thank Dr. Alfred Goldberg and Dr. Shenhav Cohen for their advice and assistance on ubiquitin and myofibrillar protein extraction. We would also like to thank Tom Giddings and Christina Clarissa for assistance with electron microscopy, Jennifer Aveena, and Massimo Buvoli and Kristen Barthel for critical reading of the manuscript.

Financial Support

This work was supported by an NIH grant (2RO1HL050560 to L.A. Leinwand), a pre-doctoral fellowship from the American Heart Association (0810037Z to P.F. Cosper) and a grant from the National Heart Lung and Blood Institute (3T32GM008497-S1 to P.F. Cosper).

References

1. Tisdale MJ. Cachexia in cancer patients. Nat Rev Cancer. 2002; 2:862–71. [PubMed: 12415256]
2. De Blaauw I, Deutz NE, Von Meyenfeldt MF. Metabolic changes in cancer cachexia--first of two parts. Clin Nutr. 1997; 16:169–76. [PubMed: 16844595]
3. Baracos VE, Reiman T, Mourtzakis M, Gioulbasanis I, Antoun S. Body composition in patients with non-small cell lung cancer: a contemporary view of cancer cachexia with the use of computed tomography image analysis. Am J Clin Nutr. 91:1133S–7S. [PubMed: 20164322]
4. Hendifar A, Yang D, Lenz F, et al. Gender disparities in metastatic colorectal cancer survival. Clin Cancer Res. 2009; 15:6391–7. [PubMed: 19789331]
5. Koo JH, Jalaludin B, Wong SK, Kneebone A, Connor SJ, Leong RW. Improved survival in young women with colorectal cancer. Am J Gastroenterol. 2008; 103:1488–95. [PubMed: 18510616]
6. al-Azzawi F, Wahab M. Estrogen and colon cancer: current issues. Climacteric. 2002; 5:3–14. [PubMed: 11974557]

7. Acharyya S, Ladner KJ, Nelsen LL, et al. Cancer cachexia is regulated by selective targeting of skeletal muscle gene products. J Clin Invest. 2004; 114:370–8. [PubMed: 15286803]
8. Tisdale MJ. Biology of cachexia. J Natl Cancer Inst. 1997; 89:1763–73. [PubMed: 9392617]
9. Smith KL, Tisdale MJ. Increased protein degradation and decreased protein synthesis in skeletal muscle during cancer cachexia. Br J Cancer. 1993; 67:680–5. [PubMed: 8471425]
10. Temparis S, Asensi M, Taillandier D, et al. Increased ATP-ubiquitin-dependent proteolysis in skeletal muscles of tumor-bearing rats. Cancer Res. 1994; 54:5568–73. [PubMed: 7923198]
11. Lecker SH, Solomon V, Mitch WE, Goldberg AL. Muscle protein breakdown and the critical role of the ubiquitin-proteasome pathway in normal and disease states. J Nutr. 1999; 129:227S–37S. [PubMed: 9915905]
12. Khal J, Hine AV, Fearon KC, Dejong CH, Tisdale MJ. Increased expression of proteasome subunits in skeletal muscle of cancer patients with weight loss. Int J Biochem Cell Biol. 2005; 37:2196–206. [PubMed: 16125116]
13. Baracos VE, DeVivo C, Hoyle DH, Goldberg AL. Activation of the ATP-ubiquitin-proteasome pathway in skeletal muscle of cachectic rats bearing a hepatoma. Am J Physiol. 1995; 268:E996–1006. [PubMed: 7539218]
14. Gottdiener JS, Gross HA, Henry WL, Borer JS, Ebert MH. Effects of self-induced starvation on cardiac size and function in anorexia nervosa. Circulation. 1978; 58:425–33. [PubMed: 679432]
15. Pruznak AM, Hong-Brown L, Lantry R, et al. Skeletal and cardiac myopathy in HIV-1 transgenic rats. Am J Physiol Endocrinol Metab. 2008; 295:E964–73. [PubMed: 18713959]
16. Hill JA, Olson EN. Cardiac plasticity. N Engl J Med. 2008; 358:1370–80. [PubMed: 18367740]
17. Burch GE, Phillips JH, Ansari A. The cachetic heart. A clinico-pathologic, electrocardiographic and roentgenographic entity. Dis Chest. 1968; 54:403–9. [PubMed: 5698585]
18. Tessitore L, Costelli P, Bonetti G, Baccino FM. Cancer cachexia, malnutrition, and tissue protein turnover in experimental animals. Arch Biochem Biophys. 1993; 306:52–8. [PubMed: 8215420]
19. Stauffer BL, Konhilas JP, Luczak ED, Leinwand LA. Soy diet worsens heart disease in mice. J Clin Invest. 2006; 116:209–16. [PubMed: 16395406]
20. Zhu H, Tannous P, Johnstone JL, et al. Cardiac autophagy is a maladaptive response to hemodynamic stress. J Clin Invest. 2007; 117:1782–93. [PubMed: 17607355]
21. Butler-Browne GS, Whalen RG. Myosin isozyme transitions occurring during the postnatal development of the rat soleus muscle. Dev Biol. 1984; 102:324–34. [PubMed: 6200371]
22. Cohen S, Brault JJ, Gygi SP, et al. During muscle atrophy, thick, but not thin, filament components are degraded by MuRF1-dependent ubiquitylation. J Cell Biol. 2009; 185:1083–95. [PubMed: 19506036]
23. Powell SR, Davies KJ, Divald A. Optimal determination of heart tissue 26S-proteasome activity requires maximal stimulating ATP concentrations. J Mol Cell Cardiol. 2007; 42:265–9. [PubMed: 17140599]
24. Tanaka Y, Eda H, Tanaka T, et al. Experimental cancer cachexia induced by transplantable colon 26 adenocarcinoma in mice. Cancer Res. 1990; 50:2290–5. [PubMed: 2317817]
25. Sharma A, Greenman J, Walker LG, Monson JR. Differences in cytokine levels due to gender in colorectal cancer patients. Cytokine. 50:91–3. [PubMed: 20116278]
26. Wakeling AE, Dukes M, Bowler J. A potent specific pure antiestrogen with clinical potential. Cancer Res. 1991; 51:3867–73. [PubMed: 1855205]
27. Jalil JE, Doering CW, Janicki JS, Pick R, Shroff SG, Weber KT. Fibrillar collagen and myocardial stiffness in the intact hypertrophied rat left ventricle. Circ Res. 1989; 64:1041–50. [PubMed: 2524288]
28. Thiedemann KU, Holubarsch C, Medugorac I, Jacob R. Connective tissue content and myocardial stiffness in pressure overload hypertrophy. A combined study of morphologic, morphometric, biochemical, and mechanical parameters. Basic Res Cardiol. 1983; 78:140–55. [PubMed: 6223618]
29. Belizario JE, Lorite MJ, Tisdale MJ. Cleavage of caspases-1, -3, -6, -8 and -9 substrates by proteases in skeletal muscles from mice undergoing cancer cachexia. Br J Cancer. 2001; 84:1135–40. [PubMed: 11308266]

30. Samarel AM. Hemodynamic overload and the regulation of myofibrillar protein degradation. Circulation. 1993; 87:1418–20. [PubMed: 8462166]
31. VanBuren P, Harris DE, Alpert NR, Warshaw DM. Cardiac V1 and V3 myosins differ in their hydrolytic and mechanical activities in vitro. Circ Res. 1995; 77:439–44. [PubMed: 7614728]
32. Tardiff JC, Hewett TE, Factor SM, Vikstrom KL, Robbins J, Leinwand LA. Expression of the beta (slow)-isoform of MHC in the adult mouse heart causes dominant-negative functional effects. Am J Physiol Heart Circ Physiol. 2000; 278:H412–9. [PubMed: 10666070]
33. Lecker SH, Jagoe RT, Gilbert A, et al. Multiple types of skeletal muscle atrophy involve a common program of changes in gene expression. Faseb J. 2004; 18:39–51. [PubMed: 14718385]
34. Solomon V, Goldberg AL. Importance of the ATP-ubiquitin-proteasome pathway in the degradation of soluble and myofibrillar proteins in rabbit muscle extracts. J Biol Chem. 1996; 271:26690–7. [PubMed: 8900146]
35. Solomon V, Baracos V, Sarraf P, Goldberg AL. Rates of ubiquitin conjugation increase when muscles atrophy, largely through activation of the N-end rule pathway. Proc Natl Acad Sci U S A. 1998; 95:12602–7. [PubMed: 9770532]
36. Wing SS, Chiang HL, Goldberg AL, Dice JF. Proteins containing peptide sequences related to Lys-Phe-Glu-Arg-Gln are selectively depleted in liver and heart, but not skeletal muscle, of fasted rats. Biochem J. 1991; 275 (Pt 1):165–9. [PubMed: 2018472]
37. Mammucari C, Milan G, Romanello V, et al. FoxO3 controls autophagy in skeletal muscle in vivo. Cell Metab. 2007; 6:458–71. [PubMed: 18054315]
38. Barth S, Glick D, Macleod KF. Autophagy: assays and artifacts. J Pathol. 2010; 221:117–24. [PubMed: 20225337]
39. Zhou X, Wang JL, Lu J, et al. Reversal of Cancer Cachexia and Muscle Wasting by ActRIIB Antagonism Leads to Prolonged Survival. Cell. 142:531–43. [PubMed: 20723755]
40. Artaza JN, Reisz-Porszasz S, Dow JS, et al. Alterations in myostatin expression are associated with changes in cardiac left ventricular mass but not ejection fraction in the mouse. J Endocrinol. 2007; 194:63–76. [PubMed: 17592022]
41. Welsh DC, Dipla K, McNulty PH, et al. Preserved contractile function despite atrophic remodeling in unloaded rat hearts. Am J Physiol Heart Circ Physiol. 2001; 281:H1131–6. [PubMed: 11514279]
42. Korte FS, Herron TJ, Rovetto MJ, McDonald KS. Power output is linearly related to MyHC content in rat skinned myocytes and isolated working hearts. Am J Physiol Heart Circ Physiol. 2005; 289:H801–12. [PubMed: 15792987]
43. Earl CA, Laurent GJ, Everett AW, Bonnin CM, Sparrow MP. Turnover rates of muscle protein in cardiac and skeletal muscles of dog, fowl, rat and mouse: turnover rate related to muscle function. Aust J Exp Biol Med Sci. 1978; 56:265–77. [PubMed: 708319]
44. Liu Z, Miers WR, Wei L, Barrett EJ. The ubiquitin-proteasome proteolytic pathway in heart vs skeletal muscle: effects of acute diabetes. Biochem Biophys Res Commun. 2000; 276:1255–60. [PubMed: 11027619]
45. Nakai A, Yamaguchi O, Takeda T, et al. The role of autophagy in cardiomyocytes in the basal state and in response to hemodynamic stress. Nat Med. 2007; 13:619–24. [PubMed: 17450150]
46. Tannous P, Zhu H, Nemchenko A, et al. Intracellular protein aggregation is a proximal trigger of cardiomyocyte autophagy. Circulation. 2008; 117:3070–8. [PubMed: 18541737]
47. Gerard KW, Schneider DL. Evidence for degradation of myofibrillar proteins in lysosomes. Myofibrillar proteins derivatized by intramuscular injection of N-ethylmaleimide are sequestered in lysosomes. J Biol Chem. 1979; 254:11798–805. [PubMed: 500675]
48. Bachmann J, Ketterer K, Marsch C, et al. Pancreatic cancer related cachexia: influence on metabolism and correlation to weight loss and pulmonary function. BMC Cancer. 2009; 9:255. [PubMed: 19635171]
49. Palomares MR, Sayre JW, Shekar KC, Lillington LM, Chlebowski RT. Gender influence on weight-loss pattern and survival of nonsmall cell lung carcinoma patients. Cancer. 1996; 78:2119–26. [PubMed: 8918405]

50. Brown M, Ning J, Ferreira JA, Bogener JL, Lubahn DB. Estrogen receptor-alpha and -beta and aromatase knockout effects on lower limb muscle mass and contractile function in female mice. Am J Physiol Endocrinol Metab. 2009; 296:E854–61. [PubMed: 19176355]

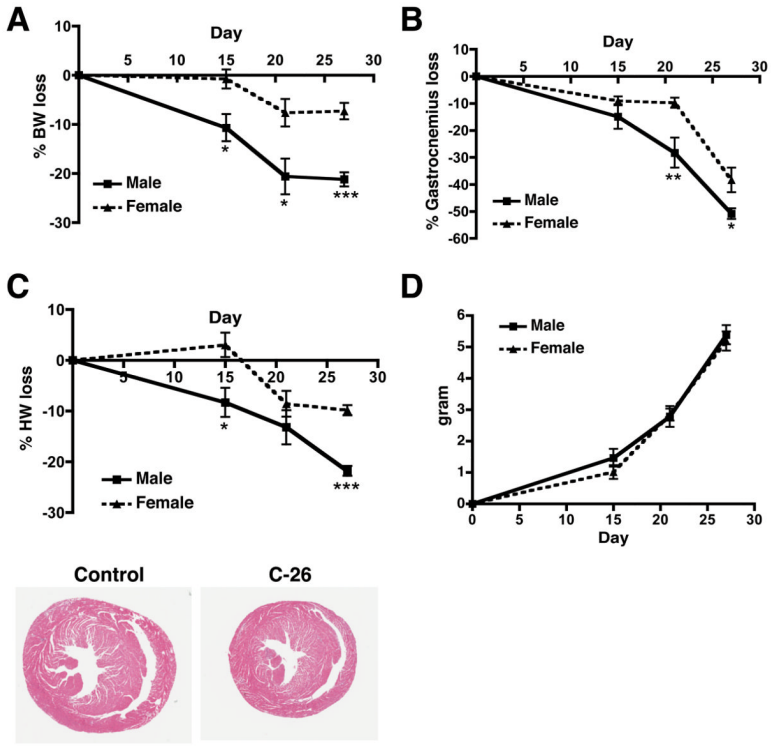

Figure 1.

Colon-26 adenocarcinoma causes cardiac muscle mass loss and body weight loss in a sexually dimorphic manner. (**A**) Percent body weight loss in male and female tumor-bearing mice. Body weight loss was calculated as the final body weight minus the tumor weight and was compared to the body weight of age-matched control mice. (**B**) Percent skeletal muscle mass (gastrocnemius) loss in male and female tumor-bearing mice. (**C**) Percent cardiac mass loss in male and female tumor-bearing mice. H&E stain of male hearts 27 days post-tumor cell inoculum (bottom). (**D**) Tumor mass in male and female mice. n = 6–8 per group. Graphs are mean ± SEM. *p < 0.05, **p < 0.01, ***p < 0.0001 vs. female.

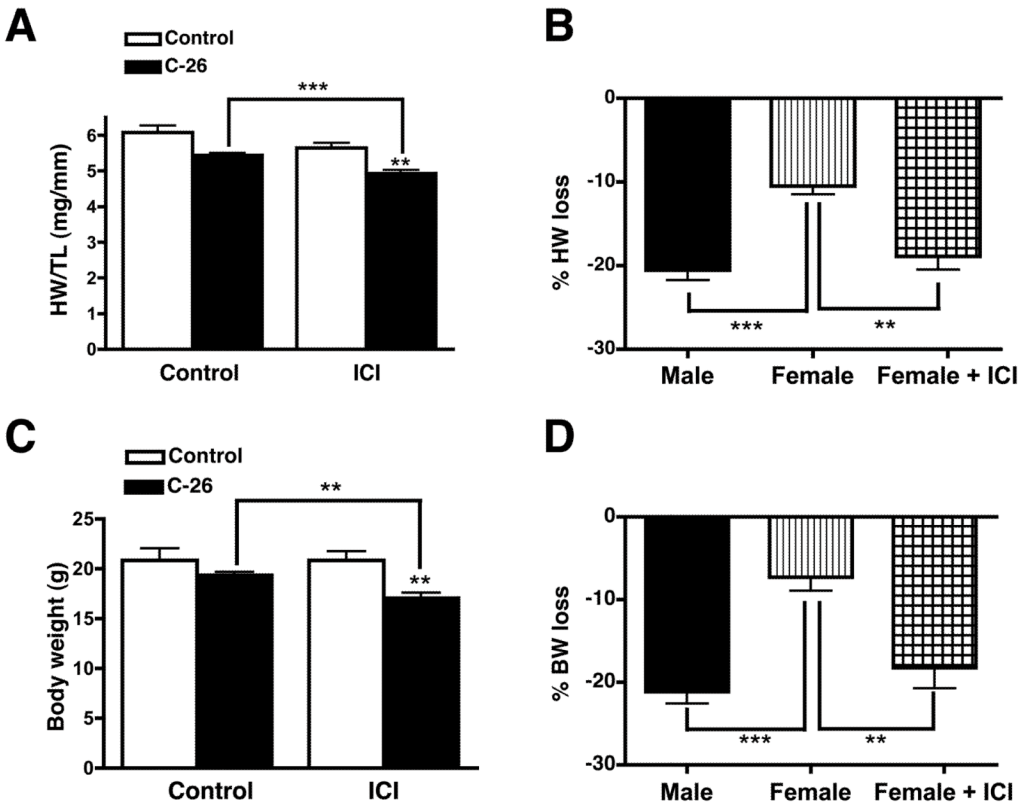

Figure 2.

Estrogen receptor signaling is required for the maintenance of cardiac and body mass in female tumor-bearing mice. Fulvestrant treatment does not affect cardiac mass (**A**) or body weight (**C**) in control mice. Inhibition of estrogen signaling in tumor-bearing females results in equivalent cardiac mass (**B**) and body weight (**D**) loss as tumor-bearing males. % loss in ICI group was calculated relative to the non-ICI controls. Heart weight (HW) is normalized to tibia length (TL) to normalize for mouse age and size. $n = 6$ per group. Graphs are mean ± SEM. $^{**}p < 0.01$, $^{***}p < 0.0001$.

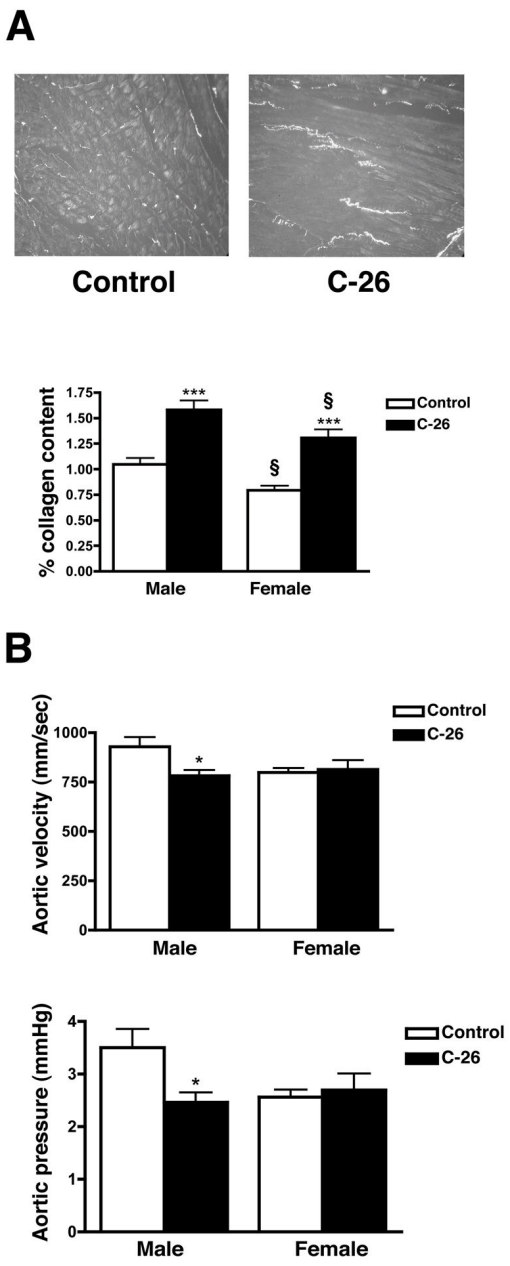

Figure 3.

Atrophic hearts have increased fibrosis and decreased function. (**A**) Picrosirius red staining of male hearts 27 days post-tumor cell inoculum. Collagen fibers appear as bright spots. Both male and female atrophic hearts have increased fibrosis (lower panel). (**B**) Echocardiography of male mice at day 27 showed significantly decreased aortic velocity and pressure, while female mice did not have any functional deficits. $n = 6$ per group. Mean ± SEM. *$p < 0.05$, ***$p < 0.0001$ vs. control. § indicates significance compared to males in each respective treatment group.

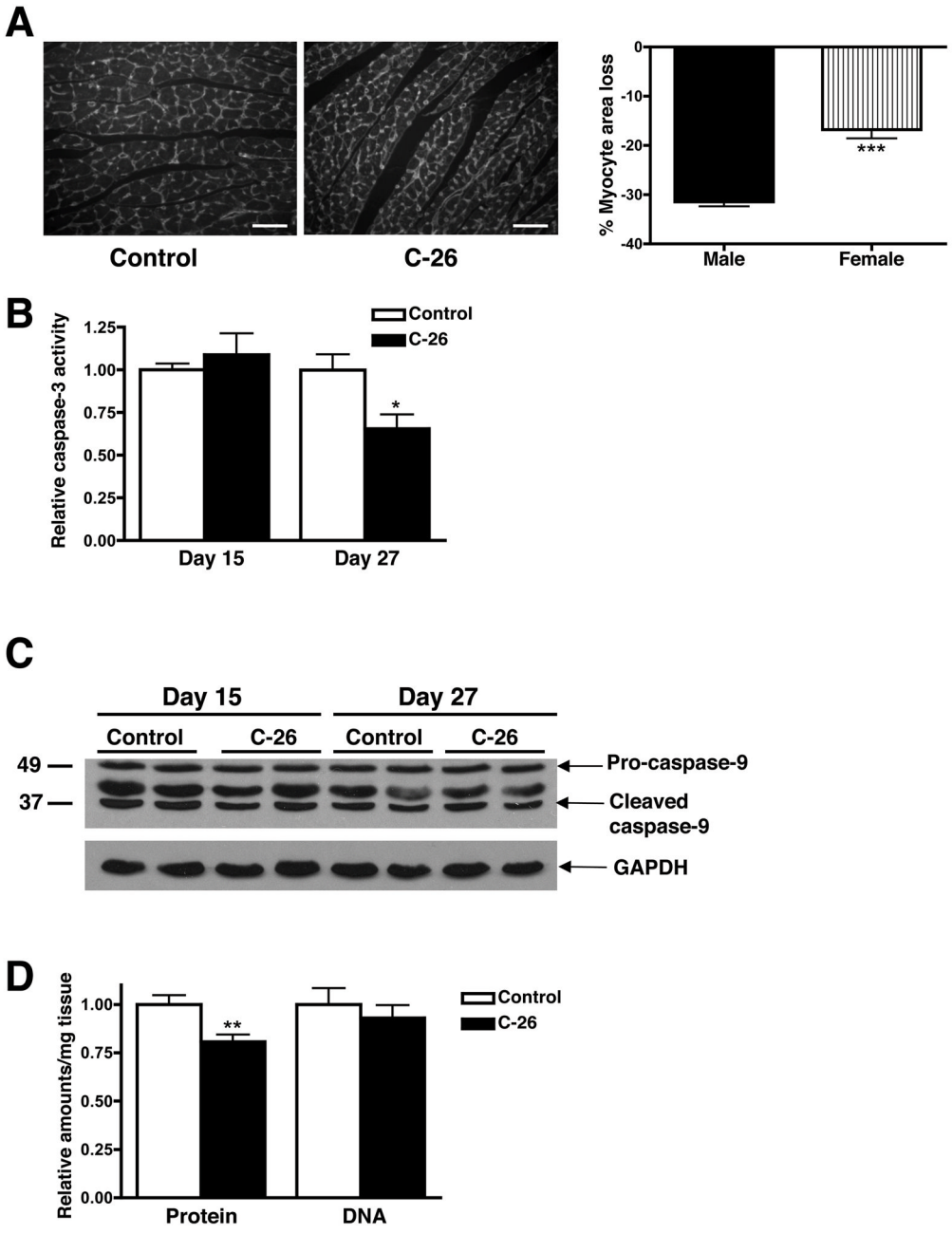

Figure 4.

Cancer-induced cardiac atrophy is due to a decrease in myocyte size and not an increase in apoptosis. (**A**) Immunohistochemistry of transverse sections of control and atrophic (day 27) male hearts with WGA. Scale bar: 300μm. At least 150 myocytes per heart (*n* = 3 per group) were quantified. (**B**) Caspase-3 activity in cardiac myocytes from male tumor-bearing mice. *n* = 5 per group. (**C**) Pro-caspase-9 and caspase-9 cleavage products did not change in atrophic hearts. (**D**) Protein and DNA content per mg of cardiac tissue. *n* = 8 per group. Mean ± SEM. *p < 0.05, ***p < 0.0001.

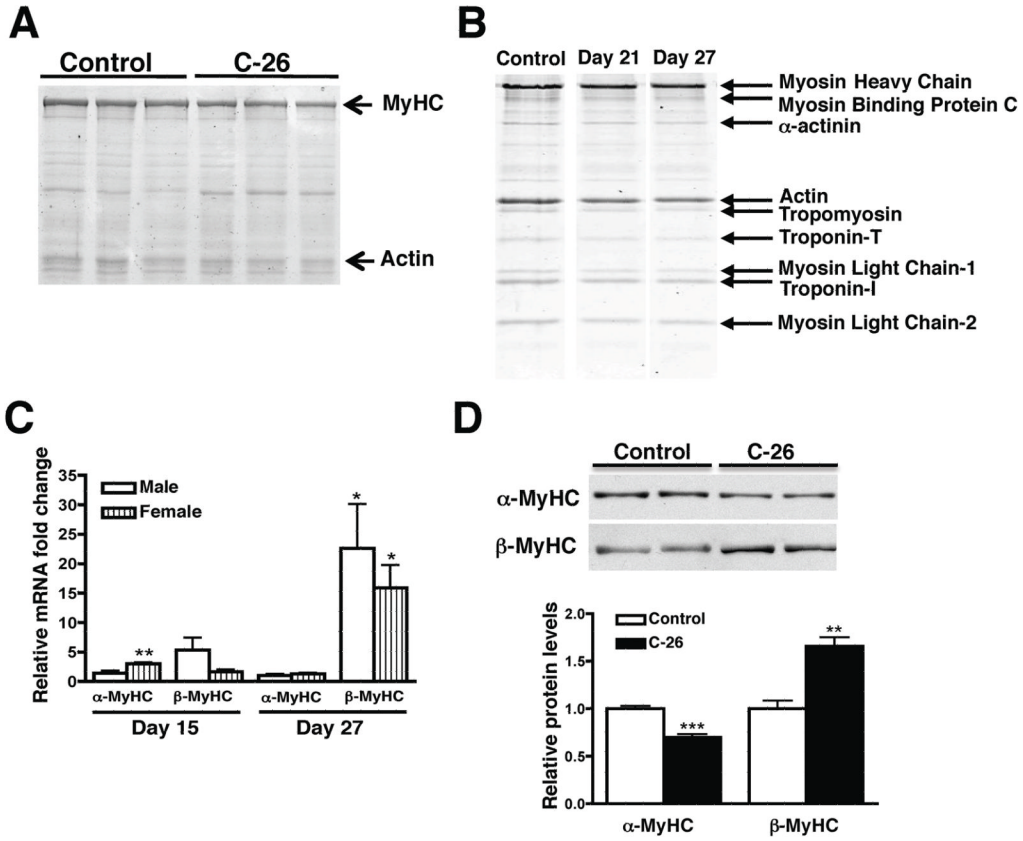

Figure 5.

All sarcomeric proteins are decreased in atrophic hearts. (**A**) Coomassie-stained gel (0.005% final cardiac mass) shows MyHC and actin levels decrease in parallel in atrophic hearts. (**B**) SDS-PAGE of purified myofibrils revealed that all sarcomeric proteins decrease in parallel during cardiac atrophy. Samples were run on the same gel but were noncontiguous. (**C**) Fold change of MyHC mRNA (normalized to 18S expression) in each sex compared to controls. (**D**) α- and β-MyHC protein expression in males at day 27. MyHC was solubilized in a high salt buffer and 0.5 μg was loaded. It was therefore not possible to re-probe the blot for a loading control. Mean ± SEM. *p < 0.05, **p < 0.01, ***p < 0.0001 vs. control. *n* = 4–5 per group.

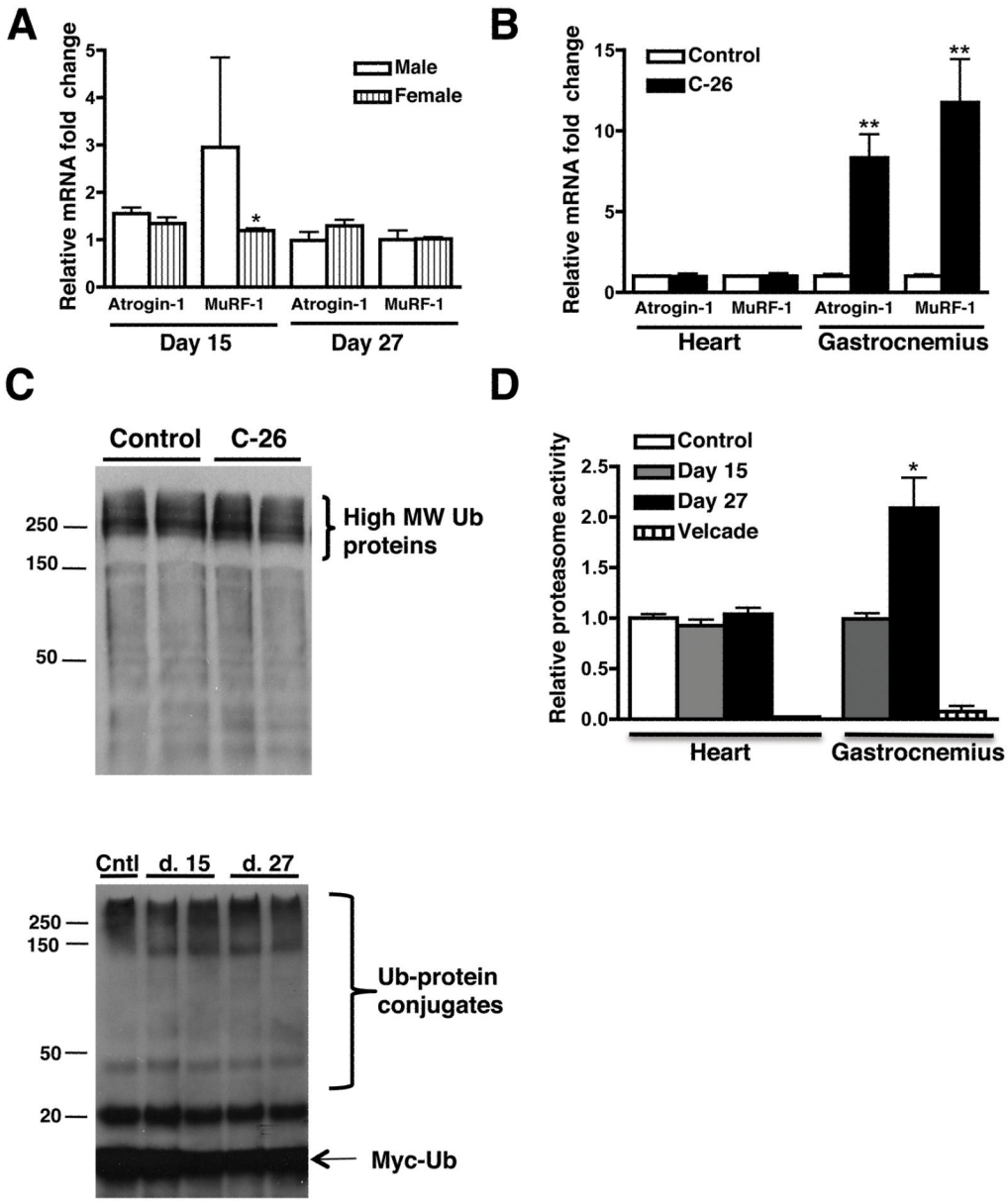

Figure 6.

Atrogin-1 and MuRF-1 expression levels do not change in atrophic hearts, but are significantly upregulated in atrophic skeletal muscle. (**A**) Atrogin-1 and MuRF-1 mRNA fold changes (normalized to 18S expression) in male and female control and atrophic hearts. (**B**) Relative atrogin-1 and MuRF-1 gene expression at day 27 in male heart and skeletal muscle (gastrocnemius). (**C**) Western blot of day 15 cardiac muscle lysates for total ubiquitin. Lower panel: Ubiquitin conjugation assays do not show a difference in ubiquitination activity between groups. (**D**) Proteasome activity in atrophic cardiac and skeletal muscle. Velcade is a potent and specific proteasome inhibitor. $n = 4$ per group. Mean ± SEM. *$p < 0.05$, **$p < 0.01$ vs. control.

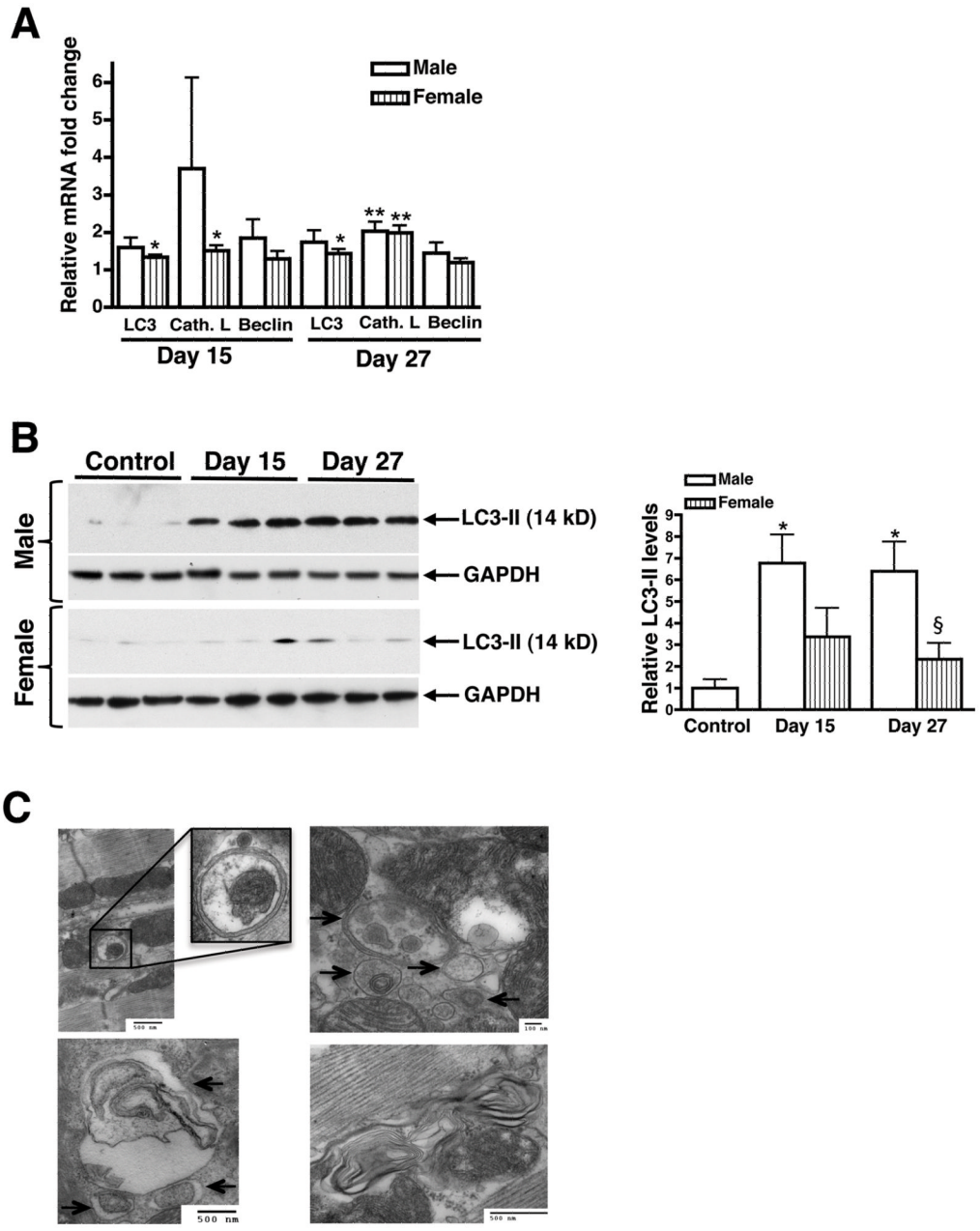

Figure 7.

Autophagy is upregulated in male and female atrophic hearts and is nearly three-fold higher in males. (**A**) Fold change of autophagy marker transcripts (normalized to 18S) in male and female atrophic hearts at days 15 and 27. (**B**) Western blots revealed increases in LC3-II levels in the hearts of both male and female tumor-bearing mice, though it was only significant in males. Quantification represents the band density of blots containing males and females on the same gel (not shown). *n* = 4 per group. (**C**) Electron micrographs from the left ventricle of tumor-bearing males (day 27). Atrophic hearts contain numerous autolysosomes and double-membraned autophagosomes (arrows) containing cellular components. Mean ± SEM. *p < 0.05, **p < 0.01, ***p < 0.0001 vs. control. § indicates significance compared to males.